Overexpression of a gibberellin 20-oxidase gene in the xylem of poplar caused an increase in nanocellulose diameter and improved paper properties

Xiaopeng Peng[a,b], Botong Tong[a,c], Jongcheol Lee[d], Kun Wang[e], Xiaojuan Yu[e], Xiong Huang[a], Jialong Wen[e], Mohamadamin Makarem[d], Hongying Pang[a], Subin Hinjan[f], Xiaojing Yan[a], Shuangquan Yao[g], Fachuang Lu[h], Baichen Wang[i], Feng Peng[e], John Ralph[h], Seong H. Kim[d], Ronald R. Sederoff[c,j], Quanzi Li[a*]

[a]State Key Laboratory of Tree Genetics and Breeding, Chinese Academy of Forestry, Beijing 100091, China
[b]Research Institute of Forestry, Chinese Academy of Forestry, Beijing 100091, China
[c]State Key Laboratory of Tree Genetics and Breeding, Northeast Forestry University, Harbin 150040, China
[d]Department of Chemical Engineering and Materials Research Institute, The Pennsylvania State University, University Park, PA 16802, USA
[e]College of Materials Science and Technology, Beijing Forestry University, Beijing 100083, China
[f]Bangkok Cordyceps Co., Ltd, Thanyaburi, Pathumthani 12130, Thailand
[g]Guangxi Key Laboratory of Clean Pulp & Papermaking and Pollution Control, College of Light Industry and Food Engineering, Guangxi University, Nanning 530004, China
[h]Department of Biochemistry and DOE Great Lakes Bioenergy Research Center, Wisconsin Energy Institute, University of Wisconsin, Madison, Wisconsin, WI 53726, USA
[i]Key Laboratory of Photobiology, Photosynthesis Research Center, Institute of Botany, Chinese Academy of Science, Beijing 100093, China
[j]Forest Biotechnology Group, Department of Forestry and Environmental Resources, North Carolina State University, Raleigh NC 27695, USA

[*] Correspondence to: Quanzi Li, State Key Laboratory of Tree Genetics and Breeding, Chinese Academy of Forestry, Beijing, 100091, China
Email address: Quanzi Li (liqz@caf.ac.cn)

Keywords: nanocellulose microfibril, poplar, gibberellin, pulp

ABSTRACT

Cellulose, the major component of secondary cell walls, is the most abundant renewable long-chain polymer on earth. Nanocellulose has become a prominent nano-reinforcement agent for polymer matrices in various industries. We report the generation of transgenic hybrid poplar overexpressing the *Arabidopsis gibberellin 20-oxidase1* gene driven by a xylem-specific promoter to increase gibberellin (GA) biosynthesis in wood. X-ray diffraction (XRD) and sum frequency generation spectroscopic (SFG) analyses showed that cellulose in transgenic trees was less crystalline, but the crystal size was larger. The nanocellulose fibrils prepared from transgenic wood had an increased diameter compared to those from wildtype. When such fibrils were used as a reinforcing agent in sheet paper preparation, the mechanical strength of the paper was significantly enhanced. Engineering the GA pathway can therefore affect nanocellulose properties, providing a new strategy for expanding nanocellulose applications.

1. Introduction

Cellulose is the principal component of both primary cell walls (PCWs) and secondary cell walls (SCWs) in plants. It is a linear polymer of β-1,4-linked glucans that aggregate to form microfibrils through intermolecular hydrogen bonds. Cellulose microfibrils are synthesized at the plasma membrane by the cellulose synthase (CESA) complex (CSC), proposed to have 18-24 CESA subunits (Gopal et al., 2015; Nixon et al., 2016; Thomas et al., 2013). During PCW deposition, the organization of cellulose microfibrils directs the orientation of cell expansion to control the growth and shape of cells (Paradez, Wright & Ehrhardt, 2006). After the PCW is formed, some cells, such as fiber cells and vessels in angiosperm stems, continue to form SCWs, inside which the interactions between cellulose, hemicelluloses and lignin produce a layered composite that enhances mechanical strength of the SCW. The SCWs are major resources for construction, pulp and paper, and textile fibers, and so on. SCWs contain a high concentration (40-50%) of cellulose, which is a versatile renewable material for chemical conversions, leading to wide applications of cellulosic biomass in industry and household products (Klemm, Heublein, Fink & Bohn, 2010).

Nanocellulose is cellulose in the form of nanostructures with lateral dimension less than 100 nm. Nanocellulose has three sub-categories, cellulose nanocrystals (CNC), nanofibrillated cellulose (NFC), and bacterial nanocellulose (BNC), based on their synthesis, morphology, and other properties (Klemm et al., 2011). Due to its renewability, biodegradability, hydrophilicity, mechanical strength, and large surface area, nanocellulose is a promising material for industrial, technological, and biomedical applications (Bacakova et al., 2019; Klemm, Heublein, Fink & Bohn, 2010; Klemm et al., 2011; Trache et al., 2016). The high length-to-diameter ratio of nanocellulose is ideal to maximize interactions with surrounding matrix elements through hydrogen bonds, which enhances paper strength (Kajanto & Kosonen, 2012). The abundant hydroxyl groups exposed at the surface can be modified to give other properties, extending its potential industrial applications.

Gibberellin (GA) is an important hormone controlling plant growth and development, including seed germination, embryogenesis, root and shoot elongation, and flowering (Schwechheimer, 2011). Since 1940, ‘the Green Revolution’ has

substantially increased yields in staple crops. Genes that contribute to the 'green revolution' effects encode enzymes in the GA biosynthetic pathway and in the response to GAs (Hedden, 2002; Peng et al., 1999). In the GA biosynthetic pathway, seven enzymes, including *ent*-copalyl diphosphate synthase (CPS), *ent*-kaurene synthase (KS), ent-kaurenoic acid oxidase (KAO), ent-kaurene oxidase (KO), GA 20-oxidase (GA20ox), GA3ox, and GA2ox, catalyze trans-geranylgeranyl diphosphate (GGDP) to produce a variety of tetracyclic diterpenoid GA forms (Sakamoto et al., 2004) (Fig. 1A). Among these products, GA_1, GA_3, GA_4 and GA_7 are the major bioactive GAs (Binenbaum, Weinstain & Shani, 2018; Sun, 2011). GA20ox is a key enzyme in GA biosynthesis. *GA20ox* antisense transgenic *Arabidopsis* has a reduced abundance of GA_4 and is a semi-dwarf, whereas *GA20ox* overexpression promotes *Arabidopsis* growth (Coles, Croker, García-Lepe, Lewis & Hedden, 1999; Huang, Raman, Ram, Fujiwara, Cerny & Brown, 1998; Zi, Mafu & Peters, 2014).

GA is also an important factor controlling wood formation. A spray of GA stimulated cambial activity and increased xylem development (Digby & Wareing, 1966; Falcioni et al., 2018; Wareing, 1958). GA_1 and GA_4 are predominantly located in the zone of expansion of xylem cells, supporting its role in xylem differentiation (Israelsson, Sundberg & Moritz, 2005). Increased GA biosynthesis in trees by *GA20ox* overexpression promotes growth and increases biomass production, and increased xylem fiber length in transgenic trees (Cho et al., 2019; Eriksson, Israelsson, Olsson & Moritz, 2000; Jeon, Cho, Park, Han, Choi & Ko, 2016; Mauriat & Moritz, 2009). GA could relieve the interactions between SLR1 (a DELLA repressor of GA signaling) and NACs (master regulators of SCW formation), promoting cellulose biosynthesis (Huang et al., 2015). Since GA is the important hormone for regulating the biosynthetic process of cellulose, it is anticipated to play an important role on determining the cellulose structures, and then extending the potential application in high-value-added fields.

Herein, the effects of GA on cellulose properties in wood were investigated in this paper, aiming to provide a novel function of GA on the crystallization and deposition of cellulose by overexpressing GA20 oxidase gene in poplar. The nanocellulose components were further extracted and comparatively studies, not only on

physicochemical properties, but also on the application in paper production as additive, expecting to prove the potential of nanocellulose from engineered wood to improve paper properties.

2. Materials and methods

2.1. Transgenic production

The *AtGA20ox1* (AT4G25420) gene encoding gibberellin 20-oxidase1 was amplified from *Arabidopsis* cDNA with the primers ArGA20F (5′-TGCAGGATCCATGGCCGTAAGTTTCGTAAC-3′) and ArGA20R (5′-TGCAGAGCTCTTAGATGGGTTTGGTGAGCC-3′) and cloned into the pGEM@-T easy vector (Promega) for sequencing. The gene was excised from the pGEM-T easy vector by *BamH*I/*Sac*I and inserted into pBI121 and pBI121-GT8D1P (Li et al., 2011), generating 35SP-GA20ox1 and 8D1P-GA20ox1, respectively. The vector constructs were transformed into *Agrobacterium tumefaciens* GV3101 and used for plant transformation of *P. alba* × *P. galandulosa*.

2.2. Reverse Transcription-quantitative PCR (*RT-qPCR*)

The differentiating xylem collection, total RNA extraction, and RT-qPCR analysis were conducted following our previous protocols (Wang et al., 2021). The primers used are ArGA20rF (5′-GGACGCTTCTCCACCAAGCT-3′) and ArGA20rR (5′-GTCCCAACGCATCGCAGAAG-3′).

2.3. Fiber length measurement

Stem xylem pieces were boiled in water until they sank. The pieces were bleached in a mixture of equal volumes of 30% hydrogen peroxide and glacial acetic acid at 60 °C for about 4 h. After samples were bleached, they were rinsed with distilled water several times. The fibers were separated from each other by shaking. After staining with 10 g/L safranin, the length of 50 fibers was measured using an Olympus BX51 light microscope.

2.4. Wood chemical composition determination

Air-dried wood was ground with mills FW135 (Tianjin TaiSiTe Instrument Co. Ltd) and DFT-50A (Wenling LinDa Machinery Co. Ltd). Wood particles of 40~60 mesh

were extracted with benzene/ethanol (2:1, v/v) for 10h. We determined the abundance and quality (Sluiter, Hames, Ruiz, Scarlata & Templeton, 2008) of cellulose, hemicelluloses and lignin. Cellulose and hemicelluloses were quantified by the HPAEC chromatography (Dinoex ICS3000) equipped with an AS50 autosampler, an ion exchange CarbopacTM PA-20 column (3 mm×150 mm, Dionex), a pulsed amperometric detector, and a PA-20 column (3 mm×30 mm, Dionex). High purity of D-(+)-glucose, D-(+)-xylose, D-(+)-galactose, D-(+)-arabinose, D-(+)-mannose, glucuronic acid and galacturonic acid were used as standards for calibration. Prior to injection, samples were filtered through 0.2 μm nylon filters (Millipore), and a volume of 25 μL was loaded onto the column, which was pre-equilibrated with 250 mM NaOH, and eluted with Milli-Q water at a flow rate of 1.1 mL min^{-1} with a gradient of water for 45 min, 200 mM NaOH for 15 min and water for 15 min.

2.5. Quantitation of endogenous GAs

The contents of endogenous GAs were determined at Wuhan MetWare Biotechnology Co., Ltd according to a reported method with minor modifications (Chen et al., 2012). Developing xylem was collected, frozen immediately in liquid nitrogen, and stored at -80 °C. Plant materials were ground to powder using a mill (NM400, Retsch). The powder (100 mg) was extracted in 1mL 80% (v/v) methanol at 4 °C overnight, and each internal standard ($[^2H_2]GA_1$, $[^2H_2]GA_3$, $[^2H_2]GA_4$, $[^2H_2]GA_7$, $[^2H_2]GA_8$, $[^2H_2]GA_9$, $[^2H_2]GA_{20}$ and $[^2H_2]GA_{34}$) was added at 1ng/g before extraction. The extract solution was passed through the tandem SPE cartridges containing 50mg C18 sorbent and 200mg SAX sorbent, which was preconditioned with 8 mL H_2O, 8mL methanol, and 8 mL 80% methanol. The C18 cartridge was removed, and the SAX cartridge was washed with 2 mL 80% methanol. The eluent, collected using 3 mL acetonitrile containing 1% formic acid, was evaporated under a mild nitrogen stream at 40 °C and dissolved in 100 μL H_2O. The resulting solution was acidified with formic acid and extracted twice with 1 mL ether. The ether phase was dried under nitrogen gas and dissolved in 100 μL acetonitrile. 10 μL triethylamine (TEA) (20 μmol/mL) and 10 μL 3-bromoacteonyltrimethylammonium (BTA) bromide (20 μmol/mL) were added. The reaction solution was vortexed for 30 min at room temperature, evaporated under

194 nitrogen, and re-dissolved in 200 µL 90% acetonitrile. A 10µL aliquot was analyzed
195 using UPLC-MS/MS (Thermo Scientific Ultimate 3000-Thermo Scientific TSQ
196 Quantiva), equipped with a Waters AXQUITY UPLC BEH C18 column. The mobile
197 phases are (A) Water with 0.04% formic acid and (B) acetonitrile with 0.04% acetic
198 acid. The program for the gradient is 90:10 (A:B, V/V) at 0 min, 85:15 at 20.0 min,
199 60:40 at 20.0min, 20:80 at 22.0 min with flow rate of 0.35 mL/min and temperature at
200 40 °C.

201 *2.6. X-ray Diffraction (XRD)*

202 Each sample was the bottom fragment of stems, which were ground with mills
203 (FW135 and DFT-50A) to 40-60 mesh powders. The powder samples were extracted
204 with benzene/ethanol (2:1) for 10 h and dried in a hood. Powder X-ray diffraction (XRD)
205 measurements were carried out using an XRD-6000 instrument (Shimadzu).

206 *2.7. Sum frequency generation (SFG) spectroscopy*

207 Transverse microtome sections of 15 µm were prepared from the bottom part of
208 stem (without bark) of 2-year-old field-grown trees. SFG analysis was as previously
209 described (Abbas et al., 2020).

210 *2.8. Nanocellulose extraction*

211 Nanocellulose was prepared using TEMPO-mediated oxidation (Kuramae, Saito &
212 Isogai, 2014). Wood powders (10 g) were suspended in 1 L H_2O with TEMPO (0.16 g)
213 and NaBr (12.7 g). TEMPO-mediated oxidation was started by adding 12% NaOCl
214 solution in the prepared mixture, and adjusted to pH 10.0 using 0.1 M HCl. This process
215 was carried out at RT with continuous strong stirring (500 rpm) for 12 h. During the
216 reaction, the pH of the system was maintained at 10-10.5 by addition of 0.5 M NaOH.
217 After washing and redispersing, the nanocellulose was obtained by ultrasonication of
218 the TEMPO-oxidized sample for 1 h at 500 W. The resulting suspension was
219 determined for the concentration to be 2 mg/mL and stored at 4 °C before use.

220 *2.9. Scanning Electron Microscope (SEM)*

221 Nanocellulose was made at a consistency of 0.002 wt% and sonicated to achieve a
222 uniform dispersion. A few drops of nanocellulose suspension were deposited onto a
223 glass slide or ultra-thin carbon type-A 400 mesh copper grids (Ted Pella). The

nanocellulose suspension was vacuum-dried and observed via scanning electron microscopes (EM8000 and EM8100, Beijing KYKY TECHNOLOGY CO. Ltd), under the acceleration voltage of 10 kV and 15 kV for imaging and 200 kV for diffraction in BF mode.

2.10. Atomic force microscopy (AFM)

Nanocellulose suspension was prepared by further dilution with distilled water (0.01wt%) to allow measuring individual CNC from the AFM images, and a few drops were deposited onto a freshly cleaved mica plate (30 mm × 12 mm) and vacuum dried. AFM imaging was conducted using a scanning probe microscope (SPM) 9600 (Shimadzu). Images of at least ten different regions of the mica plate were scanned for each sample, and no image processing except flattening was applied. Both amplitude and deflection images were collected simultaneously in tapping mode in air using commercial silicon cantilevers (Shimadzu) with a nominal frequency of 300 kHz and a nominal spring constant of 40 N m^{-1}.

2.11. Transmission electron microscopy (TEM)

2.12. Lignin structural analysis by NMR

Lignins were prepared using wood powders (40-60 mesh) following a previous protocol (Kim & Ralph, 2010) with modifications. Extract-free wood powders were subjected to two rounds of milling (450rpm, 30 min milling, 10 min rest) in a ball mill (Fritsch GmbH), and enzymatic hydrolysis use cellulolytic enzymes, followed by washing with dH_2O and then air-drying. Double enzymatic lignin (DEL, 60 mg) was dissolved in DMSO-d_6. 2-D HSQC experiment was acquired with a Bruker Avance 400 MHz spectrometer using the standard pulse sequence hsqcetgpsi and with a spectral width of 4,000 Hz and 20000 Hz for proton and carbon dimensions respectively, 64 scans, a data matrix of 1024 × 256 points, a recycle delay of 2.0 s and with an average $^1J_{C–H}$ coupling constant set to 145 Hz.

2.12. Sheet preparation and characterization

Cellulose pulp was obtained by disintegration of 1.8 g (dry weight) pulp board and 200 mL water using a lab pulp disintegrator (SKZ1025, SKZ Industrial) for 20 min. After a nanocellulose suspension was obtained (18 mL, 1 wt%), it was dispersed using

a high-energy ultrasonicator for 10 min. The cellulose pulp was dispersed for another 10 min. Then, the collected mixture was used to prepare a sheet using a British sheet former (Deju Vu Lab and Test Equipment Inc.) following the ISO standard 5269-2 (2004). The sheets were stored in a weather chamber at 23 ℃ and 50% humidity for at least 24 h.

The sheet samples were shaped into a strip of 60×5 mm for mechanical testing. The tensile strength was measured by an MTS Criterion Mode 43 from MTS Systems Corporation (Eden Prairie) following ISO standard 1924–3 (2014). The bursting strength was measured in a digital hydraulic board burst tester (Messmer Büchel) according to ISO standard 2759. To measure the cross-directional short span compressive strength, a short span compression tester (Messmer Büchel) was used and tested according to TAPPI T-826.

3. Results

3.1. Transgenic poplar overexpressing AtGA20ox1

To study the effects of GA on wood properties, we selected *AtGA20ox1*, the only *GA20ox* gene expressed in *Arabidopsis* stems (Phillips et al., 1995; Rieu et al., 2008), for overexpression in *P. alba* × *P. glandulosa* using two promoters, the CAMV 35S promoter and the xylem-specific *glycosyltransferase 8D1* (GT8D1) promoter (Li et al., 2011). The transgenic lines, named 35S and 8D1, were maintained in a growth room. Faster growth was observed for both transgenics compared to wildtype (WT) (Fig. S1, table S1). When the transgenics were moved to a field on campus, nearly half of the 35S transgenics died, whereas all 8D1 transgenics survived. Root growth was more severely affected in the *PdGA20ox1* overexpression transgenics with the 35S promoter than plants modified by the xylem-specific promoter (Jeon, Cho, Park, Han, Choi & Ko, 2016). Our study also showed that the 8D1 transgenics displayed better tolerance than the 35S transgenics when they were subjected to a sudden undesirable environment, which may be due to effects on root growth. 8D1 transgenics were selected for further analysis. The fiber cells in 8D1 transgenics had increased length compared to those in WT (Fig. S2), consistent with the previous study (Eriksson, Israelsson, Olsson & Moritz,

2000).

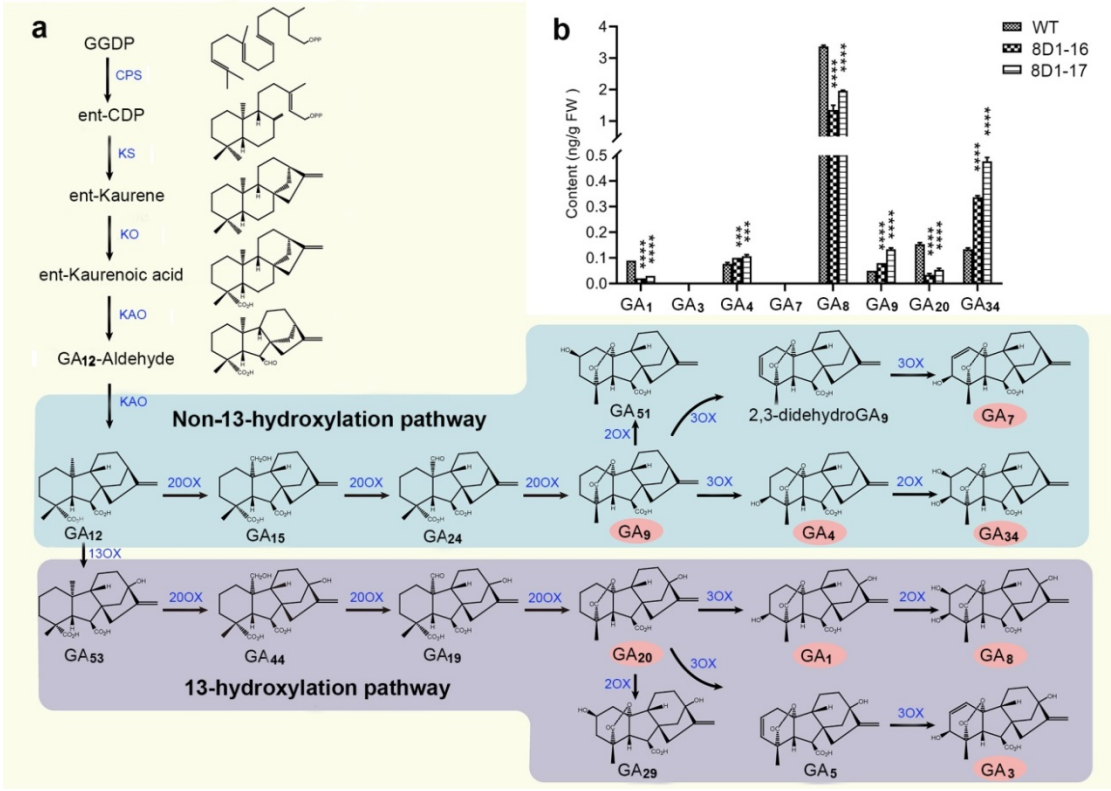

Fig. 1. Increased gibberellin biosynthesis by *AtGA20ox1* overexpression in the differentiating xylem of poplar. (a) Gibberellin biosynthetic pathway. The pathway for biosynthesis of some active GAs, and their catabolic fates, are shown. GA_{34}, GA_{51}, GA_{29}, and GA_8 are catabolic products of GA. The basic structure of *ent*-gibberellane with the numbering system of the carbons is shown at the top. GGPP, geranylgeranyl diphosphate; CPP, *ent*-copalyl diphosphate. (b) Quantification of GAs in the differentiating xylem of wildtype (WT) and transgenic poplar lines 16 (8D1-16) and 17 (8D1-17), in which *AtGA2ox1* was driven by a xylem-specific *PtrGT8D1* promoter. Asterisks indicate significant differences by Dunnett's multiple comparisons test (***, $P < 0.001$, ****, $P < 0.0001$).

RT-qPCR confirmed the overexpression of *AtGA20ox1* in the differentiating xylem of 8D1 transgenics (Fig. S3). We determined the content of 8 GAs in the differentiating xylem of lines 16 and 17 (named 8D1-16 and 8D1-17) that had the highest *AtGA20ox1* overexpression (Fig. 1B, table S2). Among the 8 GAs, GA_3 and GA_7 were undetectable. We observed an increase of GA_9, GA_4 and GA_{34} that are GA derivatives in the non-13-hydroxylation pathway, whereas the 13-hydroxylation pathway derivatives GA_{20}, GA_1 and GA_8 were decreased. Overexpression of *Arabidopsis GA20ox1* in the xylem of poplar only promoted flux in the non-13-hydroxylation pathway.

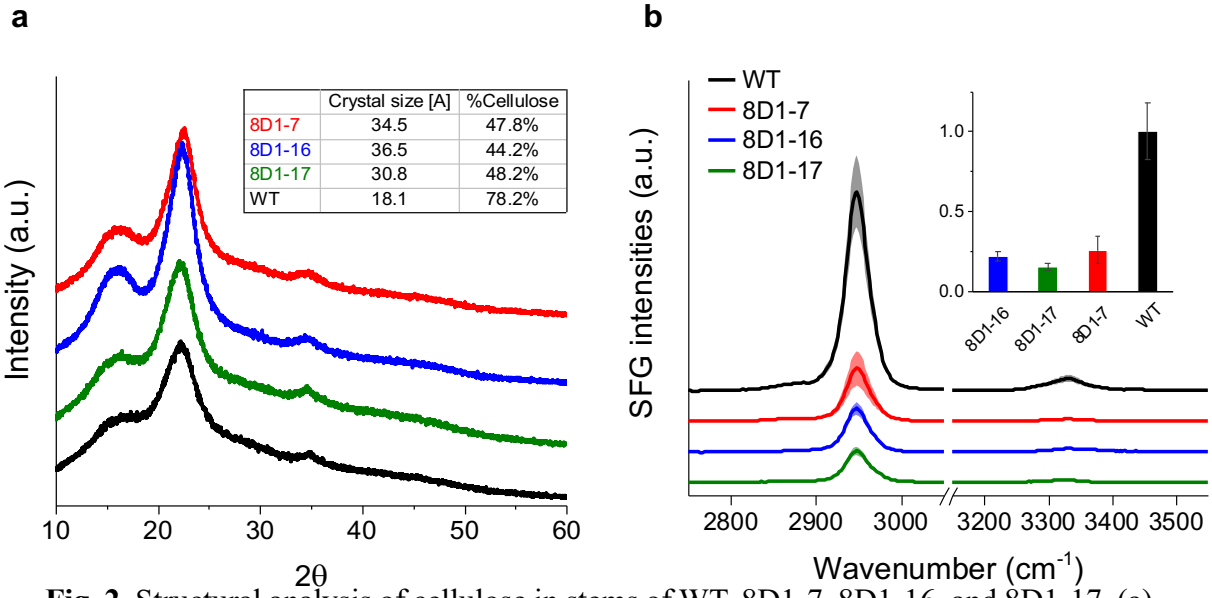

Fig. 2. Structural analysis of cellulose in stems of WT, 8D1-7, 8D1-16, and 8D1-17. (a) X-ray diffractograms of stem powders. The crystal size and crystallinity calculated from Rietveld refining (Fig. S4) are shown in the inset table. (b) SFG spectra of cellulose in cell walls. The SFG spectra were obtained by averaging hyperspectral image of 7 random areas (~50 μm × ~50 μm) of xylem fiber cell walls at per each line. The inset compares the relative area of the 2944 cm^{-1} peak, which is the characteristic mode of crystalline cellulose. Note that the XRD crystallinity and SFG intensity of cellulose do not measure the absolute amount of crystalline cellulose in the sample, but they can still be compared for qualitative trends among samples (Lee et al., 2015).

3.2. Effect on cellulose deposition by AtGA20ox1 overexpression

GA regulates cellulose synthesis through the DELLA-NAC-MYB61 cascade in rice, and GA treatment caused an increase of cellulose abundance (Huang et al., 2015). Our compositional analysis (Table 1) of the wood from 2-year-old field-grown trees showed the cellulose content in the three transgenics lines (8D1-7, -16 and -17) was 40.33-40.93%, which was slightly reduced compared to WT (44.38%). We used X-ray diffraction (XRD) to examine change in cellulose crystallinity using ground powders (Fig. 2A). The Rietveld refining of the XRD data (Fig. S4) indicated that the cellulose in transgenic trees was less crystalline, but the crystal size was larger (Table in Fig. 2A). In order to verify the decrease in XRD crystallinity, we used sum frequency generation (SFG) vibrational spectroscopy. The SFG signal intensity of cellulose in individual xylem fiber cell walls was lower in the transgenic tree stems compared to the WT (Fig. 2B). The theoretical SFG intensity calculated using the XRD crystal size and

crystallinity (Fig. S4) matched well with the experimental result.

3.3 Overexpression of GA oxidase increased nanocellulose diameter.

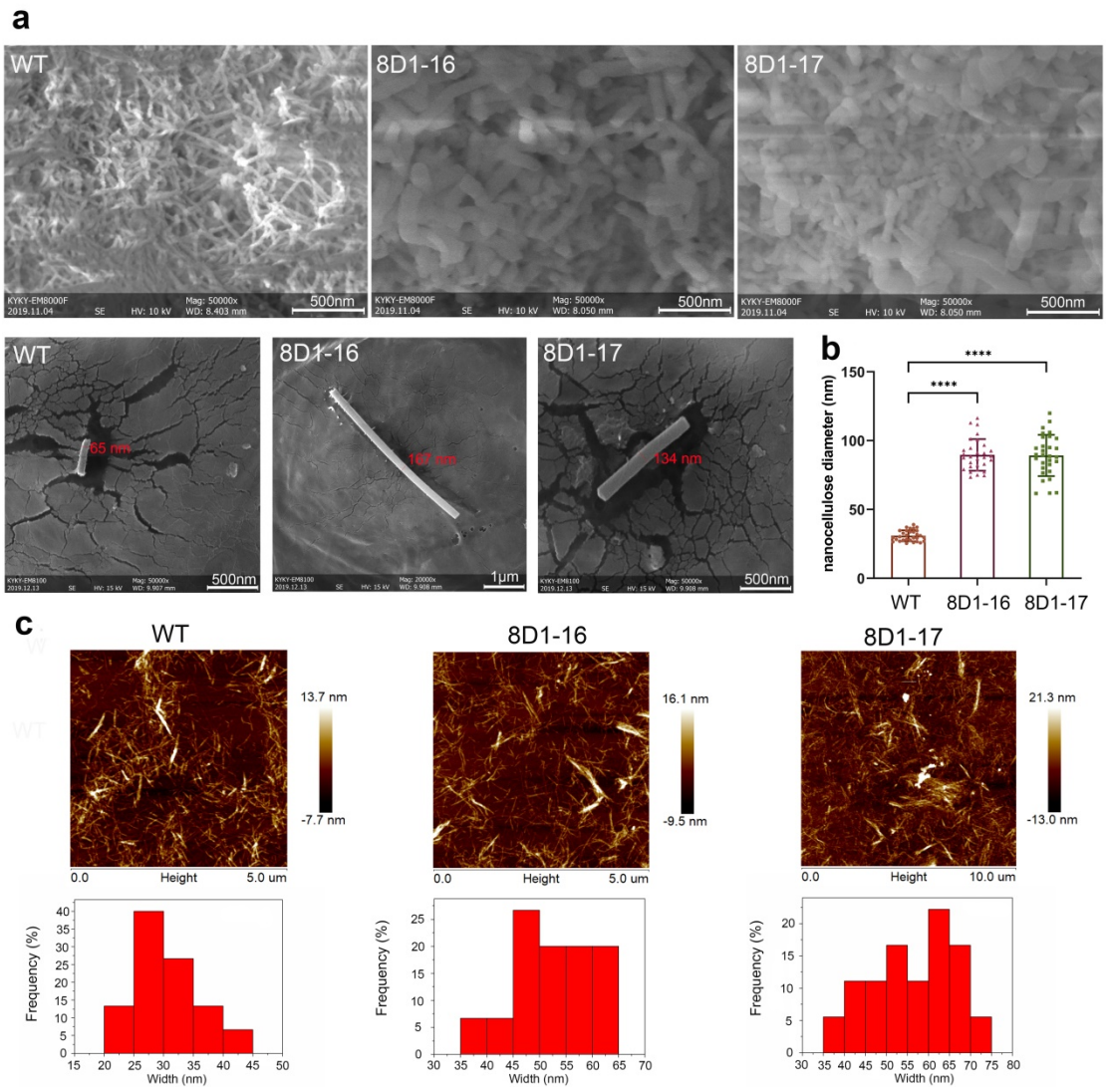

Fig. 3. Images of nanocellulose under SEM and AFM. (a) SEM images of nanocellulose from WT, 8D1-16 and 8D1-17. (b) Statistical analysis of nanocellulose diameter. (c) AMF image of nanocellulose (first layer) and their size distribution of diameter (second layer). WT: wild type; 8D1-16: Transgenic poplar line 16 of overexpression of *AtGA20ox1* using *PtrGT8D1* promoter. 8D1-17: Transgenic poplar line 17 of overexpression of *AtGA20ox1* using *PtrGT8D1* promoter. Note that in **c**, the diameters were measured from the lateral line profiles obtained with the same tip; thus the degree of tip radius artifact is the same in all three data sets.

We then prepared nanocellulose from wood powders of WT and the transgenic lines 16 and 17 using TEMPO (2,2,6,6-tetramethylpiperidine-1-oxy radical)-mediated

oxidation (Kuramae, Saito & Isogai, 2014), and obtained cellulose nanocrystals (CNCs). The CNCs were examined using scanning electron microscopy (SEM) and atomic force microscopy (AFM). The SEM images showed that nanocellulose from transgenic wood had a larger diameter than that from WT (Fig. 3A). The nanocelluloses from WT were aggregated and interlaced, and their diameter range was 25-39 nm, with a majority at 26-35 nm range, whereas the nanocellulose diameter from transgenic lines 16 and 17 ranged from 61-120 nm (Fig.3B). Under AFM, the transgenic nanocellulose had a diameter distribution of 40-70nm, whereas the diameter of WT nanocellulose varied from 20-45 nm (Fig. 3C), consistent with SEM observations.

3.3. The application of nanocellulose in improving paper properties

Nanocellulose has been used as a reinforcing agent in paper handsheet preparation. To investigate whether the increase in nanocellulose diameter improved the mechanical properties of paper, we added transgenic and WT nanocellulose into the spruce pulp at 5% loadings for sheet preparation, and measured tensile strength, bursting strength, folding endurance, and stretch strain of the papers (Batch 1 in Table 2). The tensile strength of handsheets increased from 60.1 Nm/g to 64.4 Nm/g with the addition of nanocellulose from WT, and this strength was further increased to 72.3Nm/g and 70.3 Nm/g, respectively, when the nanocellulose from 8D1-16 and 8D1-17 were added. Paper bursting strength and folding endurance were also significantly increased when the transgenic nanocellulose was added. We also observed that adding nanocellulose from WT increased paper stretch; the paper prepared with addition of transgenic nanocellulose had relatively lower stretch than the paper with WT nanocellulose however. When nanocellulose was added in recycled pulp, we also observed increased tensile strength, bursting strength, and folding endurance for the paper made with addition of transgenic nanocellulose (Batch 2 in Table 2).

3.4. Overexpression of GA oxidase resulted in increased lignin content, S/G ratio, β–O–4 and β–β linkages

We also examined the effect on lignin biosynthesis by *AtGA20ox1* overexpression. We observed that lignin content was slightly increased in the transgenic wood (Table 1). Compositional and structural characteristics of the isolated double enzymatic lignins (DELs) were analyzed by 2D-HSQC NMR (Fig. S5). For the typical linkages, β-ether, resinol, and phenylcoumaran lignin units, an increased content of β–*O*–4 and β–β

interunit linkages and a decreased content of β–5 linkages were observed in the transgenic wood. This wood had also showed an increased S/G ratio, consistent with the elevated β-ether content. The elevated S/G ratio was in agreement with the reduced amount of β-unit level in these trees (8D1-16, 8D1-17 and 8D1-7) because β–5 linkages require at least one G unit. These lignin structural changes could explain the increased saccharification in the *GA20ox* overexpression transgenic poplar following alkaline pretreatment at 120 °C (Cho et al., 2019).

4. Discussion

In this study we overexpressed a GA20 oxidase gene from *Arabidopsis*, in which this gene is a member of five in the pathway of gibberellin biosynthesis, affecting vegetative growth and early reproductive development. We investigated the effects of GA on wood formation in a poplar hybrid to observe how genetic modification of GA abundance might alter tree growth or wood formation. In previous work, overexpressing either *Arabidopsis AtGA20ox1* or *Pinus densiflora PdGA20ox1* in poplar promoted height and diameter growth, and the enhanced woody biomass features were thought to be caused by a GA-mediated increase in cambial activity (Eriksson, Israelsson, Olsson & Moritz, 2000; Jeon, Cho, Park, Han, Choi & Ko, 2016; Mauriat & Moritz, 2009). *PdGA20ox1* overexpression in a xylem-preferential pattern also promotes tree growth and biomass. We used the promoter of *PtrGT8D1*, which encodes the essential enzyme for xylan biosynthesis in SCWs, for xylem-specific overexpression of *AtGA20ox1* in a poplar hybrid, and observed increased tree growth and longer fiber cells as in previous studies (Eriksson, Israelsson, Olsson & Moritz, 2000; Jeon, Cho, Park, Han, Choi & Ko, 2016; Mauriat & Moritz, 2009). Our results confirmed that manipulation of GA biosynthesis and signal transduction is a major target for improvement in trees, to increase biomass and fiber length.

GA has been implicated in cellulose biosynthesis and cell expansion, which should influence cellulose deposition (Bringmann, Li, Sampathkumar, Kocabek, Hauser & Persson, 2012; Huang et al., 2015; Petti, Hirano, Stork & DeBolt, 2015). Although we did not observe increased cellulose biosynthesis, we observed that the overexpression

of *AtGA20ox1* increased the cellulose crystal size while decreasing the overall crystallinity. We also observed that the nanocellulose obtained from the transgenics had larger diameters than WT, indicating the novel effect of GA on cellulose deposition in wood cell walls. The increased diameter of isolated nanocellulose implicates enhanced bundling of cellulose microfibrils *in vivo*. The fact that the diameters of isolated nanocellulose fibers are significantly larger than XRD crystal size of cellulose means that TEMPO agents are not able to penetrate the space between the elementary fibrils. That could also support "more/better bundling" of cellulose microfibrils in the xylem cell walls of 8D1 transgenic trees.

Unlike the previous studies, we did not observe significantly increased cellulose biosynthesis in 8D1 transgenics. When *AtGA20ox1* was overexpressed in poplar using the CAMV 35S promoter, GAs were quantified in the internodes 7 and 8, with the upper leaves included, and both 13-hydroxylated C19 GAs (GA_1, GA_{20} and GA_8) and non-13-hydroxylaed GAs (GA_4, GA_9 and GA_{34}) were increased (Eriksson, Israelsson, Olsson & Moritz, 2000). In differentiating xylem of the 8D1 transgenics, the content of non 13-hydroxylated GAs was increased, but the content of 13-hydroxylated GAs was decreased. The different effect of *AtGA20ox1* overexpression on GA biosynthesis between 35S promoter and GT8D1 promoter may be due to differential activity of promoters or different sample locations. The difference in GA biosynthesis and phenotype between 35S:AtGA20ox1 (Eriksson, Israelsson, Olsson & Moritz, 2000) and 8D1:AtGA20ox transgenic indicated that different GA forms may have different functions. Elevation of GA_4, the major biologically active GA, in the differentiating xylem in the transgenics, supports its role in promoting fiber cell elongation. It is possible that GA_4 plays a role in the bundling of cellulose microfibrils, and that the decreased cellulose crystallinity is caused by the decrease of GA_1. Further investigations may be needed to elucidate the specific roles of the biologically active GAs during wood formation.

Nanocellulose may be employed as a thickening agent or stabilizer during papermaking (Boufi, Gonzalez, Delgado-Aguilar, Tarres, Pelach & Mutje, 2016) for its hydrophilic property, facilitating the distribution of fibers in aqueous solution. Addition

of nanocellulose at 1% and 2% significantly increased the tensile strength of paper (Kajanto & Kosonen, 2012). With the addition of 5% TEMPO-oxidized nanocellulose in laboratory CTMP handsheets, the bursting strength and tensile index were increased by almost 200% and 20%, respectively (Heijnesson Hulten, Basta, Samuelsson, Greschik, Ander & Daniel, 2012). Our study confirmed that the addition of nanocellulose from WT could improve paper properties. As compared to the nanocellulose from WT, the nanocellulose from the transgenic poplar hybrid displayed further improvements on the paper mechanical properties. Except paper stretch was reduced, and this reduction could be attributed to the shorter length of nanocellulose from GA transgenics. The major characteristic of the nanocellulose from the GA transgenics was the larger diameter, which may be the reason for the improved tensile strength of paper upon the addition of 5% nanocellulose. Further experiments will be carried out to investigate how paper mechanical properties are improved when we use pulp made from transgenic wood in papermaking. Considering the wide ranging applications, the nanocellulose from these transgenics is promising for nanocellulose-based products, such as in biomedicine.

5. Conclusions

In this study, we observed that cellulose in *AtGA20ox1* overexpression transgenic wood had increased cellulose crystal size but with decreased overall crystallinity, demonstrating novel effects of GA on the structural properties of wood cellulose, and providing evidence to support our hypothesis that hormone GA regulate the formation of cellulose structure. Engineering of GA biosynthesis in poplar resulted in an increased diameter of isolated nanocellulose, which could provide the extra mechanical properties of the obtained paper, further expanding the application of cellulose as high-value additives. Overexpression of GA oxidase in differentiating xylem also resulted in increases in lignin content, the S/G ratio and in β–*O*–4 and β–β linkages. Further investigations are needed to elucidate the mechanism on how GAs control cellulose structures, such as crystallinity, and to assess the feasibility of different nanocellulose as composite materials in various nanocellulose-based products.

CRediT authorship contribution statement

Q.L. conceived the project; X.P., B.T., J.L., X.Yu, X.H., J.W., M.M., H.P., S.H. and X.Yan performed the experiments. K.W., S.Y., L.S., F.L., B.W., F.P., J.R., R.S., S.H.K. and Q.L. analyzed the data. X.P., S.H.K., R.R.S. and Q.L. wrote the manuscript with edits from J.R., S.H.K. and R.R.S.

Declaration of competing interest

The authors declare that they have no known competing financial interests or personal relationship that could have appeared to influence the work reported in this paper.

Data availability

All data are available in the main text or the supplementary materials.

Acknowledgments

This work was supported by the Fundamental Research Funds of Chinese Academy of Forestry (CAFYBB2022XC001 to Q.L.) and the National Key Research and Development Program (2016YFD06001030 to Q.L.). F.L. and J.R. were funded by the DOE Great Lakes Bioenergy Research Center (DOE BER Office of Science, DE-SC0018409), J.L., M.M., and S.H.K were supported by the as part of the Center for Lignocellulose Structure and Formation, an Energy Frontier Research Center funded by the U.S. Department of Energy, Office of Science, Basic Energy Sciences (award #. DESC0001090), and P.X. was sponsored by the Foundation of Guangxi Key Laboratory of Clean Pulp & Papermaking and Pollution Control, College of Light Industry and Food Engineering, Guangxi University (2021KF36).

Appendix A. Supplementary data

Supplementary material related to this article can be found, in the online version, at doi:https//do.org/

500 **Table S1.** Height and stem diameter measurements of *AtGA20ox1* overexpression
501 transgenic poplar
502 **Table S2.** Gibberellin contents in differentiating xylem
503 **Fig. S1.** *AtGA20ox1* overexpression transgenic poplar (2 months old)
504 **Fig. S2.** Effects of *AtGA20ox1* overexpression on xylem fiber length
505 **Fig. S3.** qRT-PCR analysis of *AtGA20ox1* expression in the xylem of overexpression
506 transgenics
507 **Fig. S4.** Rietveld refining of XRD data and theoretical SFG intensity calculation of
508 cellulose in transgenic (8D1-7, -16, -17) and wildtype wood
509 **Fig. S5.** Heteronuclear single-quantum coherence (HSQC) nuclear magnetic resonance
510 (NMR) spectra of double-enzyme-lignins (DELs) from *AtGA20ox1* overexpression
511 transgenic poplar wood

References

Abbas, M., Peszlen, I., Shi, R., Kim, H., Katahira, R., Kafle, K., Xiang, Z., Huang, X., Min, D., Mohamadamin, M., Yang, C., Dai, X., Yan, X., Park, S., Li, Y., Kim, S. H., Davis, M., Ralph, J., Sederoff, R. R., Chiang, V. L., & Li, Q. (2020). Involvement of *CesA4*, *CesA7-A/B* and *CesA8-A/B* in secondary wall formation in *Populus trichocarpa* wood. *Tree Physiology, 40*(1), 73-89. https://doi.org/10.1093/treephys/tpz020

Bacakova, L., Pajorova, J., Bacakova, M., Skogberg, A., Kallio, P., Kolarova, K., & Svorcik, V. (2019). Versatile application of nanocellulose: From industry to skin tissue engineering and wound healing. *Nanomaterials (Basel), 9*(2), 164. http://doi.org/10.3390/nano9020164

Binenbaum, J., Weinstain, R., & Shani, E. (2018). Gibberellin localization and transport in plants. *Trends in Plant Science, 23*(5), 410-421. http://doi.org/ 10.1016/j.tplants.2018.02.005.

Boufi, S., Gonzalez, I., Delgado-Aguilar, M., Tarres, Q., Pelach, M. A., & Mutje, P. (2016). Nanofibrillated cellulose as an additive in papermaking process: A review. *Carbohydrate Polymers, 154*, 151-166. http://doi.org/ 10.1016/j.carbpol.2016.07.117

Bringmann, M., Li, E., Sampathkumar, A., Kocabek, T., Hauser, M. T., & Persson, S. (2012). POM-POM2/cellulose synthase interacting1 is essential for the functional association of cellulose synthase and microtubules in *Arabidopsis*. *Plant Cell, 24*(1), 163-677. http://doi.org/ 10.1105/tpc.111.093575

Chen, M. L., Fu, X. M., Liu, J. Q., Ye, T. T., Hou, S. Y., Huang, Y. Q., Yuan, B. F., Yan, W., & Fe Ng, Y. Q. (2012). Highly sensitive and quantitative profiling of acidic phytohormones using derivatization approach coupled with nano-LC–ESI-Q-TOF-MS analysis. *Journal of Chromatography B, 905*, 67-74. http://doi.org/ 10.1016/j.jchromb.2012.08.005

Cho, J. S., Jeon, H. W., Kim, M. H., Vo, T. K., Kim, J., Park, E. J., Choi, Y. I., Lee, H., Han, K. H., & Ko, J. H. (2019). Wood forming tissue-specific bicistronic expression of *PdGA20ox1* and *PtrMYB221* improves both the quality and quantity of woody biomass production in a hybrid poplar. *Plant Biotechnology Journal, 17*(6), 1048-1057. http://doi.org/ 10.1111/pbi.13036

Choi, J. L., Makarem M., Huang S., Kim, H. S. (2022). Numerical simulation of vibrational sum frequency generation (SFG) intensity for noncentrosymmetric domains interspersed in amorphous matrix: A case study for cellulose in plant cell wall. *Journal of Physical Chemistry* 126, 6629-6641. http://doi.org/ 10.1021/acs.jpcb.2c03897

Coles, J. P. P., A. L., Croker, S. J., García-Lepe, R., Lewis, M. J., & Hedden, P. (1999).

Modification of gibberellin production and plant development in *Arabidopsis* by sense and antisense expression of gibberellin 20-oxidase genes. *Plant Journal, 17*(5), 547-556. http://doi.org/10.1046/j.1365-313X.1999.00410.x

Digby, J., & Wareing, P. F. (1966). The effect of applied growth hormones on cambial division and the differentiation of the cambial derivatives. *Annals of Botany, 30*(3), 539-548. http://doi.org/ 10.1093/oxfordjournals.aob.a084095

Eriksson, M. E., Israelsson, M., Olsson, O., & Moritz, T. (2000). Increased gibberellin biosynthesis in transgenic trees promotes growth, biomass production and xylem fiber length. *Nature Biotechnology, 18*, 784-788. http://doi.org/ 10.1038/77355

Falcioni, R., Moriwaki, T., de Oliveira, D. M., Andreotti, G. C., de Souza, L. A., Dos Santos, W. D., Bonato, C. M., & Antunes, W. C. (2018). Increased gibberellins and light levels promotes cell wall thickness and enhance lignin deposition in xylem fibers. *Frontiers in Plant Science, 9*, 1391. http://doi.org/ 10.3389/fpls.2018.01391

Gopal, V. V., Putnam, D. K., Zhang, Q., Petridis, L., Heller, W. T., Nixon, B. T., Haigler, C. H., Kalluri, U., Coates, L., & Langan, P. (2015). A structural study of CESA1 catalytic domain of *Arabidopsis thaliana* cellulose synthesis complex: Evidence for CESA trimers. *Plant Physiology, 170*(1), 123-135. http://doi.org/ 10.1104/pp.15.01356

Hedden, P. (2002). The genes of the Green Revolution. *Trends in Genetics, 19*(1), 5-9. http://doi.org/ 10.1016/s0168-9525(02)00009-4

Heijnesson Hulten, A., Basta, J., Samuelsson, M., Greschik, T., Ander, P., & Daniel, G. (2012). Aspect on bleaching and TEMPO-mediated oxidation of wheat straw pulp fractions. *Bioresources, 7*(3), 3051-3063. http://doi.org/ 10.15376/BIORES.7.3.3051-3063

Huang, D., Wang, S., Zhang, B., Shang-Guan, K., Shi, Y., Zhang, D., Liu, X., Wu, K., Xu, Z., Fu, X., & Zhou, Y. (2015). A gibberellin-mediated DELLA-NAC signaling cascade regulates cellulose synthesis in rice. *Plant Cell, 27*(6), 1681-1696. http://doi.org/ 10.1105/tpc.15.00015

Huang, S., Raman, A. S., Ram, J. E., Fujiwara, H., Cerny, R. E., & Brown, S. M. (1998). Overexpression of 20-oxidase confers a gibberellin overproduction phenotype in *Arabidopsis*. *Plant Physiology, 119*, 773-781. http://doi.org/ 10.1104/pp.118.3.773

Israelsson, M., Sundberg, B., & Moritz, T. (2005). Tissue-specific localization of gibberellins and expression of gibberellin-biosynthetic and signaling genes in wood-forming tissues in aspen. *Plant Journal, 44*(3), 494-504. http://doi.org/ 10.1111/j.1365-313X.2005.02547.x

Jeon, H. W., Cho, J. S., Park, E. J., Han, K. H., Choi, Y. I., & Ko, J. H. (2016). Developing xylem-preferential expression of *PdGA20ox1*, a gibberellin 20-oxidase 1 from *Pinus densiflora*, improves woody biomass production in a hybrid poplar.

Plant Biotechnology Journal, 14(4), 1161-1170. http://doi.org/ 10.1111/pbi.12484

Kajanto, I., & Kosonen, M. (2012). The potential use of micro- and nano-fibrillated cellulose as a reinforcing element in paper. *Journal of Science & Technology for Forest Products and Processes, 2*, 42-48.

Kim, H., Padmakshan, D. , Li, Y. , Rencore, J. , Hatfield, R. D. , & Ralph, J. . (2017). Characterization and elimination of undesirable protein residues in plant cell wall materials for enhancing lignin analysis by solution-state nuclear magnetic resonance spectroscopy. *Biomacromolecules*, 18, 4184-4195. http://doi.org/ 10.1021/acs.biomac.7b01223

Kim, H., & Ralph, J. (2010). Solution-state 2D NMR of ball-milled plant cell wall gels in DMSO-d_6/pyridine-d_5. *Organic & Biomolecular Chemistry, 8*(3), 576-591. http://doi.org/ 10.1039/b916070a

Klemm, D., Heublein, B., Fink, H.-P., & Bohn, A. (2010). Cellulose: fascinating biopolymer and sustainable raw material. *Angewandte Chemie International Edition in English, 44*(22), 3358-3393. http://doi.org/ 10.1002/anie.200460587

Klemm, D., Kramer, F., Moritz, S., Lindstrom, T., Ankerfors, M., Gray, D., & Dorris, A. (2011). Nanocelluloses: a new family of nature-based materials. *Angewandte Chemie International Edition in English, 50*(24), 5438-5466. http://doi.org/ 10.1002/anie.201001273

Kuramae, R., Saito, T., & Isogai, A. (2014). TEMPO-oxidized cellulose nanofibrils prepared from various plant holocelluloses. *Reactive & Functional Polymers, 85*, 126-133. http://doi.org/ 10.1016/j.reactfunctpolym.2014.06.011

Lee, C., Dazen, K., Kafle, K., Moore, A., Johnson, D. K., Park, S., & Kim, S. H. (2015). Correlations of apparent cellulose crystallinity determined by XRD, NMR, IR, Raman, and SFG methods. *Advances in Polymer Science, 271*, 115-131. http://doi.org/ 10.1007/12_2015_320

Li, Q., Min, D., Wang, J. P., Peszlen, I., Horvath, L., Horvath, B., Nishimura, Y., Jameel, H., Chang, H. M., & Chiang, V. L. (2011). Down-regulation of glycosyltransferase 8D genes in *Populus trichocarpa* caused reduced mechanical strength and xylan content in wood. *Tree Physiology, 31*(2), 226-236. http://doi.org/ 10.1093/treephys/tpr008

Mauriat, M., & Moritz, T. (2009). Analyses of *GA20ox*- and *GID1*-over-expressing aspen suggest that gibberellins play two distinct roles in wood formation. *Plant Journal, 58*(6), 989-1003. http://doi.org/10.1111/j.1365-313X.2009.03836.x

Nixon, B. T., Mansouri, K., Singh, A., Du, J., Davis, J. K., Lee, J. G., Slabaugh, E., Vandavasi, V. G., O'Neill, H., & Roberts, E. M. (2016). Comparative structural and computational analysis supports eighteen cellulose synthases in the plant cellulose synthesis complex. *Scientific Reports, 6*, 28696. http://doi.org/ 10.1038/srep28696

Paradez, A., Wright, A., & Ehrhardt, D. W. (2006). Microtubule cortical array organization and plant cell morphogenesis. *Current Opinion in Plant Biology, 9*(6), 571-578. http://doi.org/ 10.1016/j.pbi.2006.09.005

Peng, J., Richards, D. E., Hartley, N. M., Murphy, G. P., Devos, K. M., Flintham, J. E., Beales, J., Fish, L. J., Worland, A. J., Pelica, F., Sudhakar, D., Christou, P., Snape, J. W., Gale, M. D., & Harberd, N. P. (1999). 'Green_revolution' genes encode mutant gibberellin response modulators. *Nature, 400*, 256-261. http://doi.org/10.1038/22307

Petti, C., Hirano, K., Stork, J., & DeBolt, S. (2015). Mapping of a cellulose-deficient mutant named dwarf1-1 in sorghum bicolor to the green revolution gene gibberellin20-oxidase reveals a positive regulatory association between gibberellin and cellulose biosynthesis. *Plant Physiology, 169*(1), 705-716. http://doi.org/ 10.1104/pp.15.00928

Phillips, A. L., Ward, D. A., Uknes, W. S., Appleford, N. E. J., Lange, T., Huttly, A. K., Gaskin, P., Graebe, J. E., & Hedden, P. (1995). Isolation and expression of three gibberellin 20-oxidase cDNA clones from *Arabidopsis*. *Plant Physiology, 108*, 1049-1057. http://doi.org/ 10.1104/pp.108.3.1049

Rieu, I., Ruiz-Rivero, O., Fernandez-Garcia, N., Griffiths, J., Powers, S. J., Gong, F., Linhartova, T., Eriksson, S., Nilsson, O., Thomas, S. G., Phillips, A. L., & Hedden, P. (2008). The gibberellin biosynthetic genes *AtGA20ox1* and *AtGA20ox2* act, partially redundantly, to promote growth and development throughout the *Arabidopsis* life cycle. *Plant Journal, 53*(3), 488-504. http://doi.org/ 10.1111/j.1365-313X.2007.03356.x

Sakamoto, T., Miura, K., Itoh, H., Tatsumi, T., Ueguchi-Tanaka, M., Ishiyama, K., Kobayashi, M., Agrawal, G. K., Takeda, S., Abe, K., Miyao, A., Hirochika, H., Kitano, H., Ashikari, M., & Matsuoka, M. (2004). An overview of gibberellin metabolism enzyme genes and their related mutants in rice. *Plant Physiology, 134*(4), 1642-1653. http://doi.org/ 10.1104/pp.103.033696

Schwechheimer, C. (2011). Gibberellin signaling in plants – the extended version. *Frontiers in Plant Science, 2*, 107. http://doi.10.3389/fpls.2011.00107.

Sluiter, A., Hames, B., Ruiz, R. O., Scarlata, C., & Templeton, D. (2008). Determination of structural carbohydrates and lignin in biomass. *NREL Laboratory Analytical Procedures, National Renewable Energy Laboratroy, Golden, Co, USA*.

Sun, T. P. (2011). The molecular mechanism and evolution of the GA–GID1–DELLA signaling module in plants. *Current Biology, 21*(9), R338-345. http://doi.org/ 10.1016/j.cub.2011.02.036

Thomas, L. H., Forsyth, V. T., Sturcová, A., Kennedy, C. J., May, R. P., Altaner, C. M., Apperley, D. C., Wess, T. J., & Jarvis, M. C. (2013). Structure of cellulose

microfibrils in primary cell walls from collenchyma. *Plant Physiology, 161*(1), 465-476. http://doi.org/ 10.1104/pp.112.206359

Trache, D., Hussin, M. H., Hui Chuin, C. T., Sabar, S., Fazita, M. R., Taiwo, O. F., Hassan, T. M., & Haafiz, M. K. (2016). Microcrystalline cellulose: Isolation, characterization and bio-composites application-A review. *International Journal of Biological Macromolecules, 93*, 789-804. http://doi.org/ 10.1016/j.ijbiomac.2016.09.056

Wang, Q., Dai, X., Pang, H., Cheng, Y., Huang, X., Li, H., Yan, X., Lu, F., Wei, H., Sederoff, R. R., & Li, Q. (2021). BEL1-like homeodomain protein BLH6a is a negative regulator of *CAl5H2* in sinapyl alcohol monolignol biosynthesis in poplar. *Frontiers in Plant Science, 12*, 695223. http://doi.org/ 10.3389/fpls.2021.695223

Wareing, P. F. (1958). Interaction between indole-acetic acid and gibberellic acid in cambial activity. *Nature, 181*, 1744-1745. http://doi.org/ 10.1038/1811744a0

Zi, J., Mafu, S., & Peters, R. J. (2014). To gibberellins and beyond! Surveying the evolution of (di)terpenoid metabolism. *Annual Review of Plant Biology, 65*, 259-286. http://doi.org/ 0.1146/annurev-arplant-050213-035705

Figure legends

Fig. 1. Increased gibberellin biosynthesis by *AtGA20ox1* overexpression in the differentiating xylem of poplar. (a) Gibberellin biosynthetic pathway. The pathway for biosynthesis of some active GAs, and their catabolic fates, are shown. GA_{34}, GA_{51}, GA_{29}, and GA_8 are catabolic products of GA. The basic structure of *ent*-gibberellane with the numbering system of the carbons is shown at the top. GGPP, geranylgeranyl diphosphate; CPP, *ent*-copalyl diphosphate. (b) Quantification of GAs in the differentiating xylem of wildtype (WT) and transgenic poplar lines 16 (8D1-16) and 17 (8D1-17), in which *AtGA2ox1* was driven by a xylem-specific *PtrGT8D1* promoter. Asterisks indicate significant differences by Dunnett's multiple comparisons test (***, $P < 0.001$, ****, $P < 0.0001$).

Fig. 2. Structural analysis of cellulose in stems of WT, 8D1-7, 8D1-16, and 8D1-17. (a) X-ray diffractograms of stem powders. The crystal size and crystallinity calculated from Rietveld refining (fig. S4) are shown in the inset table. (b) SFG spectra of cellulose in cell walls. The SFG spectra were obtained by averaging hyperspectral image of 7 random areas (~50 μm ×~50 μm) of xylem fiber cell walls at per each line. The inset compares the relative area of the 2944 cm^{-1} peak, which is the characteristic mode of

crystalline cellulose. Note that the XRD crystallinity and SFG intensity of cellulose do not measure the absolute amount of crystalline cellulose in the sample, but they can still be compared for qualitative trends among samples (Lee et al., 2015).

Fig. 3. Images of nanocellulose under SEM and AFM. (a) SEM images of nanocellulose from WT, 8D1-16 and 8D1-17. (b) Statistical analysis of nanocellulose diameter. (c) AMF image of nanocellulose (first layer) and their size distribution of diameter (second layer). WT: wild type; 8D1-16: Transgenic poplar line 16 of overexpression of *AtGA20ox1* using *PtrGT8D1* promoter. 8D1-17: Transgenic poplar line 17 of overexpression of *AtGA20ox1* using *PtrGT8D1* promoter. Note that in **c**, the diameters were measured from the lateral line profiles obtained with the same tip; thus the degree of tip radius artifact is the same in all three data sets.

Table 1. Wood composition of *AtGA20ox1* overexpression transgenic *P. alba* × *P. glandulosa*

Lines	Cellulose	Hemicelluloses						Lignin		
		Arabinan	Galactan	Xylan	Mannan	Galacturonic acid	Glucuronic acid	Acid soluble	Acid insoluble	Total lignin
WT	44.38±0.44	1.15±0.02	1.28±0.01	11.58±0.10	0.19±0.01	1.60±0.02	2.15±0.02	5.44±0.36	16.25±0.97	21.69±0.60
8D1-7	40.93±1.45*	1.08±0.02**	1.18±0.05*	12.19±0.23*	0.23±0.01**	1.63±0.02	2.09±0.02*	6.26±0.02*	17.80±0.23	24.06±0.24**
8D1-16	40.33±0.21***	1.09±0.01**	1.14±0.01***	12.53±0.06***	0.25±0.01***	1.67±0.01**	2.08±0.01**	6.23±0.03*	18.27±0.01*	24.50±0.04**
8D1-17	40.85±0.20***	1.09±0.01**	1.15±0.01***	12.83±0.20***	0.26±0.01***	1.69±0.02**	2.09±0.02*	6.23±0.01*	18.46±0.36*	24.69±0.36**

Results are represented as value means (w/w) ± standard errors (SE). SE is based on three biological replicates. Values are expressed as weight percent based on vacuum-dried extractive free wood weight. Asterisks show significant differences by the Student's test (*, $P < 0.05$; **, $P < 0.01$; ***, $P < 0.001$). WT: wild type; 8D1-16: Transgenic poplar line 16 of overexpression of *AtGA20ox1* using the *PtrGT8D1* promoter. 8D1-17: Transgenic poplar line 17 showing overexpression of *AtGA20ox1* using the *PtrGT8D1* promoter.

Table 2. Sheet properties

		Without adding CNC	Adding CNC from WT1	Adding CNC from WT2	Adding CNC from 8D1-16	Adding CNC from 8D1-17
Batch 1 Using spruce pulp	Folding endurance (time)	161±11.55	210±7.80	170±7.20	228.2±9.50*	242±7.07**
	Tensile index (Nm/g)	60.1±0.78	64.52±0.49	64.3±0.69	70.28±1.01****	72.3±0.62****
	Stretch (mm)	2.92±0.10	3.47±0.06	3.34±0.17	2.75±0.07***	2.92±0.04*
	Bursting strength (Kpa)	234.50	242.00	241.10	255.20	251.40
Batch 2 Using recycled pulp	Folding endurance (time)	6.85±0.03	n/m	9.90±0.01	13.70±0.18****	13.29±0.15****
	Tensile index (Nm/g)	0.46±0.00	n/m	0.67±0.00	0.91±0.01**	0.89±0.00****
	Bursting strength (Kpa)	240.00	n/m	243.50	261.70	256.20

Results are represented as value means (w/w) ± standard errors (SE). SE represents at least three independent analyses, except bursting strength. Significant difference between two transgenic lines and WT was determined by Tukey's multiple comparisons test (*, $P < 0.05$; **, $P < 0.01$; ***, $P < 0.001$, ****, $P < 0.0001$). Stretch is not measured in batch 2 because the paper made from recycled pulp always broke. WT1 and WT2: wild type; 8D1-16: Transgenic poplar line 16 of overexpression of *AtGA20ox1* using *PtrGT8D1* promoter. 8D1-17: Transgenic poplar line 17 of overexpression of *AtGA20ox1* using *PtrGT8D1* promoter. n/m; not measured. The nanocellulose used for batches 1 and 2 were prepared independently.

Abbas, M., Peszlen, I., Shi, R., Kim, H., Katahira, R., Kafle, K., Xiang, Z., Huang, X., Min, D., Mohamadamin, M., Yang, C., Dai, X., Yan, X., Park, S., Li, Y., Kim, S. H., Davis, M., Ralph, J., Sederoff, R. R., Chiang, V. L., & Li, Q. (2020). Involvement of *CesA4*, *CesA7-A/B* and *CesA8-A/B* in secondary wall formation in *Populus trichocarpa* wood. *Tree Physiol., 40*(1), 73-89.

Bacakova, L., Pajorova, J., Bacakova, M., Skogberg, A., Kallio, P., Kolarova, K., & Svorcik, V. (2019). Versatile application of nanocellulose: From industry to skin tissue engineering and wound healing. *Nanomaterials (Basel), 9*(2), 164.

Binenbaum, J., Weinstain, R., & Shani, E. (2018). Gibberellin localization and transport in plants. *Trends Plant Sci., 23*(5), 410-421.

Boufi, S., Gonzalez, I., Delgado-Aguilar, M., Tarres, Q., Pelach, M. A., & Mutje, P. (2016). Nanofibrillated cellulose as an additive in papermaking process: A review. *Carbohydr. Polym., 154*, 151-166.

Bringmann, M., Li, E., Sampathkumar, A., Kocabek, T., Hauser, M. T., & Persson, S. (2012). POM-POM2/cellulose synthase interacting1 is essential for the functional association of cellulose synthase and microtubules in *Arabidopsis*. *Plant Cell, 24*(1), 163-677.

Chen, M. L., Fu, X. M., Liu, J. Q., Ye, T. T., Hou, S. Y., Huang, Y. Q., Yuan, B. F., Yan, W., & Fe Ng, Y. Q. (2012). Highly sensitive and quantitative profiling of acidic phytohormones using derivatization approach coupled with nano-LC–ESI-Q-TOF-MS analysis. *J. Chromatogr. B, 905*, 67-74.

Cho, J. S., Jeon, H. W., Kim, M. H., Vo, T. K., Kim, J., Park, E. J., Choi, Y. I., Lee, H., Han, K. H., & Ko, J. H. (2019). Wood forming tissue-specific bicistronic expression of *PdGA20ox1* and *PtrMYB221* improves both the quality and quantity of woody biomass production in a hybrid poplar. *Plant Biotechnol. J., 17*(6), 1048-1057.

Coles, J. P. P., A. L., Croker, S. J., García-Lepe, R., Lewis, M. J., & Hedden, P. (1999). Modification of gibberellin production and plant development in *Arabidopsis* by sense and antisense expression of gibberellin 20-oxidase genes. *Plant J., 17*(5), 547-556.

Digby, J., & Wareing, P. F. (1966). The effect of applied growth hormones on cambial division and the differentiation of the cambial derivatives. *Ann. Bot., 30*(3), 539-548.

Eriksson, M. E., Israelsson, M., Olsson, O., & Moritz, T. (2000). Increased gibberellin biosynthesis in transgenic trees promotes growth, biomass production and xylem fiber length. *Nat. Biotech., 18*, 784-788.

Falcioni, R., Moriwaki, T., de Oliveira, D. M., Andreotti, G. C., de Souza, L. A., Dos Santos, W. D., Bonato, C. M., & Antunes, W. C. (2018). Increased gibberellins and light levels promotes cell wall thickness and enhance lignin deposition in xylem fibers. *Front. Plant Sci., 9*, 1391.

Gopal, V. V., Putnam, D. K., Zhang, Q., Petridis, L., Heller, W. T., Nixon, B. T., Haigler, C. H., Kalluri, U., Coates, L., & Langan, P. (2015). A structural study of CESA1 catalytic domain of *Arabidopsis thaliana* cellulose synthesis complex: Evidence for CESA trimers. *Plant Physiol., 170*(1), 123-135.

Hedden, P. (2002). The genes of the Green Revolution. *Trends Genet., 19*(1), 5-9.

Heijnesson Hulten, A., Basta, J., Samuelsson, M., Greschik, T., Ander, P., & Daniel, G. (2012). Aspect on bleaching and TEMPO-mediated oxidation of wheat straw pulp fractions. *Bioresources, 7*(3), 3051-3063.

Huang, D., Wang, S., Zhang, B., Shang-Guan, K., Shi, Y., Zhang, D., Liu, X., Wu, K., Xu, Z., Fu, X., & Zhou, Y. (2015). A gibberellin-mediated DELLA-NAC signaling

cascade regulates cellulose synthesis in rice. *Plant Cell, 27*(6), 1681-1696.
Huang, S., Raman, A. S., Ram, J. E., Fujiwara, H., Cerny, R. E., & Brown, S. M. (1998). Overexpression of 20-oxidase confers a gibberellin overproduction phenotype in *Arabidopsis*. *Plant Physiol., 119*, 773-781.
Israelsson, M., Sundberg, B., & Moritz, T. (2005). Tissue-specific localization of gibberellins and expression of gibberellin-biosynthetic and signaling genes in wood-forming tissues in aspen. *Plant J., 44*(3), 494-504.
Jeon, H. W., Cho, J. S., Park, E. J., Han, K. H., Choi, Y. I., & Ko, J. H. (2016). Developing xylem-preferential expression of *PdGA20ox1*, a gibberellin 20-oxidase 1 from *Pinus densiflora*, improves woody biomass production in a hybrid poplar. *Plant Biotechnol. J., 14*(4), 1161-1170.
Kajanto, I., & Kosonen, M. (2012). The potential use of micro- and nano-fibrillated cellulose as a reinforcing element in paper. *J-FOR, 2*, 42-48.
Kim, H., & Ralph, J. (2010). Solution-state 2D NMR of ball-milled plant cell wall gels in DMSO-d_6/pyridine-d_5. *Org. Biomol. Chem., 8*(3), 576-591.
Klemm, D., Heublein, B., Fink, H.-P., & Bohn, A. (2010). Cellulose: fascinating biopolymer and sustainable raw material. *Angew. Chem. Int. Ed, 44*(22), 3358-3393.
Klemm, D., Kramer, F., Moritz, S., Lindstrom, T., Ankerfors, M., Gray, D., & Dorris, A. (2011). Nanocelluloses: a new family of nature-based materials. *Angew. Chem. Int. Ed. Engl., 50*(24), 5438-5466.
Kuramae, R., Saito, T., & Isogai, A. (2014). TEMPO-oxidized cellulose nanofibrils prepared from various plant holocelluloses. *React. Funct. Polym., 85*, 126-133.
Lee, C., Dazen, K., Kafle, K., Moore, A., Johnson, D. K., Park, S., & Kim, S. H. (2015). Correlations of apparent cellulose crystallinity determined by XRD, NMR, IR, Raman, and SFG methods. *Adv. Polym. Sci., 271*, 115-131.
Li, Q., Min, D., Wang, J. P., Peszlen, I., Horvath, L., Horvath, B., Nishimura, Y., Jameel, H., Chang, H. M., & Chiang, V. L. (2011). Down-regulation of glycosyltransferase 8D genes in *Populus trichocarpa* caused reduced mechanical strength and xylan content in wood. *Tree Physiol., 31*(2), 226-236.
Mauriat, M., & Moritz, T. (2009). Analyses of *GA20ox*- and *GID1*-over-expressing aspen suggest that gibberellins play two distinct roles in wood formation. *Plant J., 58*(6), 989-1003.
Nixon, B. T., Mansouri, K., Singh, A., Du, J., Davis, J. K., Lee, J. G., Slabaugh, E., Vandavasi, V. G., O'Neill, H., & Roberts, E. M. (2016). Comparative structural and computational analysis supports eighteen cellulose synthases in the plant cellulose synthesis complex. *Sci. Rep., 6*, 28696.
Paradez, A., Wright, A., & Ehrhardt, D. W. (2006). Microtubule cortical array organization and plant cell morphogenesis. *Curr. Opin. Plant Biol., 9*(6), 571-578.
Peng, J., Richards, D. E., Hartley, N. M., Murphy, G. P., Devos, K. M., Flintham, J. E., Beales, J., Fish, L. J., Worland, A. J., Pelica, F., Sudhakar, D., Christou, P., Snape, J. W., Gale, M. D., & Harberd, N. P. (1999). 'Green_revolution' genes encode mutant gibberellin response modulators. *Nature, 400*, 256-261.
Petti, C., Hirano, K., Stork, J., & DeBolt, S. (2015). Mapping of a cellulose-deficient mutant named dwarf1-1 in sorghum bicolor to the green revolution gene gibberellin20-oxidase reveals a positive regulatory association between gibberellin and cellulose biosynthesis. *Plant Physiol., 169*(1), 705-716.
Phillips, A. L., Ward, D. A., Uknes, W. S., Appleford, N. E. J., Lange, T., Huttly, A. K., Gaskin, P., Graebe, J. E., & Hedden, P. (1995). Isolation and expression of three gibberellin 20-oxidase cDNA clones from *Arabidopsis*. *Plant Physiol., 108*, 1049-1057.

Rieu, I., Ruiz-Rivero, O., Fernandez-Garcia, N., Griffiths, J., Powers, S. J., Gong, F., Linhartova, T., Eriksson, S., Nilsson, O., Thomas, S. G., Phillips, A. L., & Hedden, P. (2008). The gibberellin biosynthetic genes *AtGA20ox1* and *AtGA20ox2* act, partially redundantly, to promote growth and development throughout the *Arabidopsis* life cycle. *Plant J., 53*(3), 488-504.

Sakamoto, T., Miura, K., Itoh, H., Tatsumi, T., Ueguchi-Tanaka, M., Ishiyama, K., Kobayashi, M., Agrawal, G. K., Takeda, S., Abe, K., Miyao, A., Hirochika, H., Kitano, H., Ashikari, M., & Matsuoka, M. (2004). An overview of gibberellin metabolism enzyme genes and their related mutants in rice. *Plant Physiol., 134*(4), 1642-1653.

Schwechheimer, C. (2011). Gibberellin signaling in plants - the extended version. *Front. Plant Sci., 2*, 107.

Sluiter, A., Hames, B., Ruiz, R. O., Scarlata, C., & Templeton, D. (2008). Determination of structural carbohydrates and lignin in biomass. *NREL Laboratory Analytical Procedures, National Renewable Energy Laboratroy, Golden, Co, USA*.

Sun, T. P. (2011). The molecular mechanism and evolution of the GA–GID1–DELLA signaling module in plants. *Curr. Biol., 21*(9), R338-345.

Thomas, L. H., Forsyth, V. T., Sturcová, A., Kennedy, C. J., May, R. P., Altaner, C. M., Apperley, D. C., Wess, T. J., & Jarvis, M. C. (2013). Structure of cellulose microfibrils in primary cell walls from collenchyma. *Plant Physiol., 161*(1), 465-476.

Trache, D., Hussin, M. H., Hui Chuin, C. T., Sabar, S., Fazita, M. R., Taiwo, O. F., Hassan, T. M., & Haafiz, M. K. (2016). Microcrystalline cellulose: Isolation, characterization and bio-composites application-A review. *Int. J. Biol. Macromol., 93*, 789-804.

Wang, Q., Dai, X., Pang, H., Cheng, Y., Huang, X., Li, H., Yan, X., Lu, F., Wei, H., Sederoff, R. R., & Li, Q. (2021). BEL1-like homeodomain protein BLH6a is a negative regulator of *CAl5H2* in sinapyl alcohol monolignol biosynthesis in poplar. *Front. Plant Sci., 12*, 695223.

Wareing, P. F. (1958). Interaction between indole-acetic acid and gibberellic acid in cambial activity. *Nature, 181*, 1744-1745.

Zi, J., Mafu, S., & Peters, R. J. (2014). To gibberellins and beyond! Surveying the evolution of (di)terpenoid metabolism. *Annu. Rev. Plant Biol., 65*, 259-286.